Preparation, Characterization, Structure, and Dynamics of Carboxymethyl Chitosan Grafted with Acrylic Acid Sodium Salt

ARTICLE *in* JOURNAL OF APPLIED POLYMER SCIENCE · NOVEMBER 2010

Impact Factor: 1.77 · DOI: 10.1002/app.32517

2 AUTHORS, INCLUDING:

Mahdy Mohammed Elmahdy
Mansoura University
17 PUBLICATIONS **332** CITATIONS

SEE PROFILE

Preparation, Characterization, Structure, and Dynamics of Carboxymethyl Chitosan Grafted with Acrylic Acid Sodium Salt

Ibrahim M. El-Sherbiny,[1]* Mahdy M. Elmahdy[2†]

[1]*Polymer Laboratory, Chemistry Department, Faculty of Science, Mansoura University, Mansoura ET-35516, Egypt*
[2]*Physics Department, Faculty of Science, Mansoura University, Mansoura ET-35516, Egypt*

Received 16 August 2009; accepted 25 March 2010
DOI 10.1002/app.32517
Published online 11 June 2010 in Wiley InterScience (www.interscience.wiley.com).

ABSTRACT: Graft copolymerization of different vinyl monomers onto chitosan (Cs) and its derivatives can alter their properties and consequently expands their potential applications. In this study, carboxymethyl chitosan (CMCs) was prepared and characterized. Graft copolymerization of acrylic acid sodium salt (AAs) onto CMCs was accomplished by using ammonium persulphate (APS)-induced free radical polymerization in aqueous medium under nitrogen atmosphere. Occurrence of grafting was confirmed and the effects of [AAs], [APS], reaction time, and temperature on the extent of grafting were studied. The influence of grafting yield on the structure and dynamics was also investigated by using differential scanning calorimetry (DSC), two-dimensional wide-angle X-ray scattering (2D-WAXS), scanning electron microscopy (SEM), and dielectric spectroscopy. Preliminary study, using dielectric spectroscopy, was carried out to the CMCs-*g*-AAs copolymer with grafting percent $\sim$ 2900%, as an example, in a wide range of temperature (from 299 to 473 K) and frequency (from 1×10^{-2} to 1×10^{5} Hz). One relaxation process with Arrhenius type was detected. This process has the characteristics of a secondary relaxation process related to local chain dynamics with activation energy of 53 $\pm$ 3 kJ/mol. © 2010 Wiley Periodicals, Inc. J Appl Polym Sci 118: 2134–2145, 2010

Key words: molecular dynamics; carboxymethyl chitosan; acrylic acid sodium salt

INTRODUCTION

Chitosan (Cs) is a cationic polymer obtained through alkaline *N*-deacetylation of natural chitin. Chitosan is environmentally friendly material with many physical, chemical, and biological desirable characteristics.[1,2] However, its poor solubility in both water and common organic solvents limits its extensive use. Several approaches were applied for conversion of Cs into a water-soluble form. One of these approaches is the carboxymethylation. As reported in many investigations,[3,4] carboxymethyl chitosan (CMCs) has several desirable characteristics. For instance, CMCs has good ability to form films, fibers, and hydrogels. For this reason, it has been extensively used in many potential applications.[3–5]

A significant body of research has recently focused on chemical modification of Cs and its derivatives to modify their characteristics and consequently expand their potential applications.[6–8] Among various techniques of chemical modifications, graft copolymerization of vinyl monomers onto polymer backbones is one of the most helpful because it is a good and easy method for introduction of certain desired properties via selecting the appropriate types of side chains. In spite of the large number of grafting studies onto Cs,[9–12] it can be found that a relatively little published studies have discussed the graft copolymerization of vinyl monomers onto CMCs.[2,13–19] Graft copolymerization onto Cs and CMCs can be achieved in the presence of a wide range of initiator systems such as ammonium persulfate (APS), potassium persulfate (KPS), and ceric ammonium nitrate (CAN). These initiators usually generate free radical sites on polymer backbones.

A recently reported trial has studied the optimum conditions for grafting of acrylic acid (AA) onto CMCs using Ce^{+4} ions as initiator.[18] Also Xie et al. have prepared CMCs-*g*-AA using APS as initiator for studying its antibacterial activity.[19] However, the optimum conditions of grafting using APS, structural characteristics and new potential applications

**Present address:* College of Pharmacy, University of Texas in Austin, Austin, Texas 78712.
†*Present address:* Institute for Experimental Physics I, University of Leipzig, Linéestraße 5, D-04103 Leipzig, Germany.
Correspondence to: I. M. El-Sherbiny (sherbiny@mail.utexas.edu).

of the CMCs-*g*-AA copolymer still need to be investigated. In the present contribution, Cs was carboxymethylated and then graft copolymerized with the sodium salt of acrylic acid (AAs) in mild aqueous medium using APS as initiator. The grafting process has been confirmed and the effects of reaction conditions on the extent of grafting were extensively investigated. Given that the resulting copolymer of CMCs grafted with AAs owns an interesting collection of dipolar groups, dielectric spectroscopy was used, as a suitable technique to probe molecular motions with high sensitivity, to look into the dipolar fluctuations of the copolymer in broad ranges of temperature and frequency.

Dielectric spectroscopy of different polysaccharides has been reported in the literature, mainly for cellulose[20–22] and for starch.[23,24] Einfeldt et al.[25,26] have reported the different processes of a variety of polysaccharides and their interpretations. At low temperatures, they observed γ- and β-relaxations. The γ-process was attributed to the motions of local side groups in the repeating units, whereas the β-process was originated from the motions of local main chain, due to fluctuations within the glycosidic bonds. At low frequency side of the dominant β-process, Einfeldt et al.[25,26] observed an additional relaxation process and they called it a β-wet relaxation (β_{wet}) which was attributed to the motion of a mixed phase of both polysaccharide and water or other swelling solvent. This process, β_{wet}, was observed also by Montes et al.[21,27] and they called it β-relaxation. At higher temperatures (80–180°C), another process (σ-process) was observed which was attributed to proton migration.

In case of Cs, Nogales et al.[28] described two relaxation processes: (i) β-relaxation, with characteristics similar to the β-relaxation reported by Einfeldt et al.,[25,26] but was attributed to hydrogen-bonded water, and (ii) a conduction process related to adsorbed water molecules upon heating at $T > 80$°C which disappeared after water desorption at high temperatures. By using dielectric spectroscopy, Viciosa et al.[29] reported two relaxation processes with an Arrhenius temperature dependence for wet (13% of water content) and annealed (for 20 min at 150°C) non-neutralized and neutralized forms of Cs. The first process (located at temperature between −100°C and 0°C) has the characteristic of a secondary relaxation process which was related to local chain dynamics, and the second process located at higher temperatures which were related to conductivity. Recently, the same group studied the dielectric characterization of the same molecules upon drying.[30] Three relaxation processes were detected in the temperature range from −130°C up to increasing final temperature: (i) a β-wet process which was detected when the sample has a higher water content. This process has vanished after heating the sample to 150°C; (ii) a β-process, which was located at temperatures below 0°C. This process has enhanced with annealing at 150°C; and (iii) a σ-process that deviated to higher temperatures with drying. This process became more mobile in the non-neutralized form. Moreover, in dried neutralized Cs, they observed a fourth process in the low-frequency side of the secondary β-process which was diminished after annealing.

In this study, CMCs was prepared and characterized. Then graft copolymerization of acrylic acid sodium salt (AAs) onto CMCs was achieved with aid of APS in aqueous medium. Occurrence of grafting was confirmed by various ways and the effects of different reaction parameters on the extent of grafting were investigated. Moreover, the influence of grafting yield on the structure and dynamics of the synthesized copolymers was studied with aid of differential scanning calorimetry (DSC), two-dimensional wide-angle X-ray scattering (2D-WAXS), and scanning electron microscopy (SEM). Then, a preliminary study, using dielectric spectroscopy (DS), was carried out for one sample of the synthesized CMCs-*g*-AAs copolymers with grafting percent ∼ 2900%, as an example, in a wide range of temperature (from 299 to 473 K) and frequency (from 1×10^{-2} to 1×10^{5} Hz). This investigation using DS was a preliminary trial to monitor the relaxation processes, the ion mobility, and the dc-conductivity of the selected sample. The comprehensive DS study of the entire synthesized copolymers samples that investigates effect of the grafting degree onto the relaxation process, ion mobility, and dc-conductivity will be presented in more details elsewhere.

EXPERIMENTAL

Materials

Chitosan (Cs) was purchased from Acros Organics (NJ). Acrylic acid (AA), anhydrous 99%, and ammonium persulphate (APS) were supplied by Aldrich. Monochloroacetic acid was obtained from Riedel–De Haenag Seelze (Hanover, Germany). Isopropyl alcohol, acetone, methanol, acetic acid, and all other reagents were of analytical grade and used as received.

Methods

Preparation and characterization of Cs, CMCs, and graft copolymer

Characterization of Cs. The average molecular weight (M_w) of the Cs under investigation was determined to be 31.8×10^4 D using the Mark-Houwink viscometry method,[1] in a solvent of 0.1*M* acetic acid/0.2*M*

NaCl maintained at 25°C. The efflux times of both the solvent and the Cs solutions were measured with aid of Cannon-Fenske Routine Viscometer (Cannon Instrument, State College, PA). Each sample was measured thrice. Also, the *N*-deacetylation % of Cs was found to be 73.6% as determined by FTIR using the following relationship:[31]

$$\%\ N\text{-deacetylation} = 100\left[1 - \left(\frac{A_{1655}}{A_{3340}}\right)\left(\frac{1}{1.33}\right)\right] \quad (1)$$

where A is the absorbance at the given wave number. These two absorption signals (1655 and 3340 cm^{-1}) correspond to the amide and the primary amino groups of Cs, respectively. The factor (1.33) represents the value of the ratio of A_{1655}/A_{3340} for the fully *N*-acetylated Cs.

Preparation of CMCs. The water-soluble CMCs was prepared by a modified method as previously reported in our earlier work.[1] Briefly, 2 g of Cs were transferred to 500 mL RBF and suspended in 50 mL of isopropyl alcohol at room temperature for 5 h. To the swollen Cs suspension, 80 mL of aqueous NaOH solution (60% w/v) were added and then the whole mixture was refluxed at 85°C for 2 h. Then, 100 mL of aqueous monochloroacetic acid solution (60% w/v) were added over a period of 10 min. The mixture was heated with stirring, at 65°C for a further 4 h. The reaction mixture was then neutralized using HCl solution (4*M*). After removal of the undissolved residue by filtration, CMCs was precipitated by adding methanol. The product was filtered, washed several times with a mixture of CH_3OH/H_2O (1 : 1), and dried under vacuum.

The average molecular weight of the CMCs, dissolved in 0.1*M* aqueous NaCl, was estimated at 25°C using the following relationships:[32]

$$\eta_r = \frac{t}{t_0}$$
$$\eta_{sp} = \eta_r - 1$$
$$[\eta] = \frac{\left(4\eta_{sp}^{1.02} \times \ln \eta_r\right)}{C^{1.01}\left(3\eta_{sp} + \ln \eta_r\right)} \quad (2)$$
$$[\eta] = 7.92 \times 10^{-5} M_r^{1.00}$$

where t and t_0 are the delivery times of CMCs solution and the solvent, respectively, C is the concentration of CMCs (g/mL), η_r and $[\eta]$ are the relative and intrinsic viscosities, respectively. M_r is the viscosity average molecular weight of CMCs.

The substitution degree (Sd) of the prepared CMCs was also determined using potentiometric titration.[32] A solution of 150 mg of CMCs dissolved in 50 mL of distilled water was adjusted to pH < 2 by adding hydrochloric acid. The CMCs solution was then titrated with 0.1*M* aqueous NaOH and the pH value was simultaneously recorded. The NaOH amount was determined by the second-order differential method and the Sd value was calculated as follow:

$$\mathrm{Sd} = \frac{161 \times V \times C}{m_{\mathrm{CMCs}} - 58 \times V \times C} \quad (3)$$

where m_{CMCs} is the mass (g) of CMCs, V and C are the volume and molarity of NaOH solution, respectively. The values 58 and 161 represent the molecular weights of the carboxymethyl group and the glucosamine unit of Cs, respectively.

Graft copolymerization. Graft copolymerization was carried out in a 250 mL two-necked glass flask using 0.1 g CMCs. Before addition of the predetermined amount of monomer, AA, the monomer was neutralized by using NaOH (4*M*) and then completed to the desired volume by deionized water. The used monomer concentrations were in the range of (0.25–3*M*). The components were mixed through regular stirring for 30 min with bubbling of slow stream of nitrogen gas. Then the flask was placed in a thermostated oil bath at the desired reaction temperature (50–90°C). Upon reaching the desired temperature, the appropriate concentration of the initiator, APS (3–15 m*M* based on the total volume of reaction mixture) dissolved in 10 mL of deionized water was added dropwise with stirring. The graft copolymerization was continued for a predetermined period (0.5–3 h). After the desired time, the reaction was stopped by letting air into the flask and rapidly cooling down the reaction. The products were precipitated by pouring the reaction mixture into acetone. The precipitate was filtered off, washed with acetone, and the crude product was dried under vacuum and weighed. The homopolymer formed was extensively extracted in a Soxhlet apparatus by refluxing with methanol for 24 h. The residual graft copolymer obtained was washed with methanol, dried, and weighed. The percent grafting (*G*%) and the grafting efficiency (GE%) of the copolymers were calculated as follow:[33]

$$G\% = 100\left[\frac{(W_g - W_0)}{W_0}\right] \quad (4)$$

$$GE\% = 100\left[\frac{W_g}{(W_g + W_h)}\right] \quad (5)$$

where W_g, W_h, and W_0 are the weights of graft copolymer, homopolymer, and CMCs, respectively. Both *G*% and GE% represent the mean values ± SD of three independent grafting experiments.

Structure characterization

Both CMCs and CMCs-*g*-AAs copolymer were characterized by FTIR. The dried samples were pressed with KBr and their FTIR spectra were recorded on a Perkin-Elmer Paragon 1000 FTIR spectrometer within the wave number range of 4000–600 cm^{-1} at 25°C. The elemental analysis for CMCs and CMCs-*g*-AAs were performed in Carlo Erba Elemental analyzer EA 1108 using a flash combustion technique. Differential scanning calorimetry (DSC) of CMCs and CMCs-*g*-AAs copolymers of different grafting yields were performed using Perkin-Elmer DSC7 in a nitrogen atmosphere from −30°C to 300°C at scanning rate of 10°C/min. The samples (10–12 mg) were weighed into aluminum sample pans and sealed. An empty aluminum pan of approximately equal weight was used as a reference. All peaks were determined and the areas were converted into enthalpy values. The wide-angle X-ray scattering (WAXS) of powder CMCs and CMCs-*g*-AAs copolymers of different values of *G*% were investigated using 2D-WAXS equipment (Rigaku Micro Max 007 microfocus imitating anode X-ray generator (CuKα) coupled with Osmic "Blue" confocal optics and a Rigaku RAxis (VI++) image-plate detector (Massey University, NZ). Images were recorded and analyzed with Crystal Clear.[34] The surface morphology of the dried CMCs and graft copolymer was investigated by SEM (Hitachi S-800 field emission scanning electron microscope operated in secondary electron mode with a Robinson backscatter detector.). The digital image capture system that is used for obtaining the digital images is a Hitachi PCI system. Dry samples were mounted on aluminum stubs with double-sided conducting carbon tapes and coated with a 50/50 mixture of gold and palladium to minimize surface charging. The sample was scanned at an accelerating voltage of 20 kV.

Dielectric spectroscopy

The dielectric measurements were carried out on dried powder samples. The samples were dried in a vacuum oven at 100°C, then cooled down to room temperature, and then pressed into disks of 12.5 mm diameter and with a thickness of 42 μm. The common circular area of the disk surfaces was rubbed with silver past to achieve better electrode contact. A double phase rotary pump (Edward MLW, type DS8, GDR) evacuated the cell to a pressure of about 10^{-3} torr. The cell was evacuated at least 1 h after inserting the sample into it to ensure minimum humidity. The heating rate was kept uniform and slow by using a computerized temperature controller R/S Cole-Parmer instrument (Model 89000-15, accuracy ±0.1°C, USA) to avoid thermal strains. A Chromel-Alumel thermocouple (K-type) was kept close to the specimen to measure its temperature. The connecting wires were shielded cables and as short as possible to reduce wiring capacitance. The applied voltage was adjusted to 1 V to avoid thermoelectric voltage and polarization effect. A standard resistance decade box, Tech instruments (Model RD-5, Japan) was used as a pure resistance.

The dielectric measurements were made at different temperatures in the range from 299 to 473 K, at atmospheric pressure, and for frequencies in the range from 1×10^{-2} to 1×10^{5} Hz, using Stanford research systems model SR830 DSP lock-in amplifier for collecting data (frequency range 1 mHz to 102 kHz with accuracy 25 ppm + 30 μHz and resolution 4.5 digits or 0.1 mHz, phase resolution 0.01°, amplitude 4 mV_{rms} to 5 V_{rms} with 2 mV resolution, and 1% accuracy). Data were collected as heating up the sample. In each run, the sample stayed at each temperature for about 15 min to assure both stabilization and spectrum acquisition.

The complex dielectric permittivity $\varepsilon^* = \varepsilon' - i\varepsilon''$, where ε' is the real and ε'' is the imaginary part, is a function of frequency ω, temperature T, and pressure P, $\varepsilon^* = \varepsilon^*(\omega, T, P)$.[35] In the analysis of the DS spectra, the following empirical equation of Havriliak and Negami (HN)[36] was used.

$$\varepsilon^*(\mathrm{T}, P, \omega) = \varepsilon_\infty(T, P) + \frac{\Delta\varepsilon(T, P)}{[1 + (i\omega\tau_{\mathrm{HN}}(T, P))^{\alpha}]^{\gamma}} + \frac{\sigma_0(T, P)}{i\varepsilon_f\omega} \quad (6)$$

where $\varepsilon_\infty(T, P)$ is the high-frequency permittivity, $\tau_{\mathrm{HN}}(T, P)$ is the characteristic relaxation time in this equation, $\Delta\varepsilon(T, P) = \varepsilon_o(T, P) - \varepsilon_\infty(T, P)$ is the relaxation strength, α, γ (with limits $0 < \alpha, \alpha\gamma \leq 1$) describe, respectively, the symmetrical and asymmetrical broadening of the distribution of relaxation times, σ_o is the dc-conductivity, and ε_f is the permittivity of free space. From τ_{HN}, the relaxation time at maximum loss, $\tau_{\max}$, is obtained analytically from eq. (7):

$$\tau_{\max} = \tau_{\mathrm{HN}}\left[\frac{\sin\left(\frac{\pi\alpha}{2+2\gamma}\right)}{\sin\left(\frac{\pi\alpha\gamma}{2+2\gamma}\right)}\right]^{-1/\alpha} \quad (7)$$

The dielectric data in the frequency domain were fitted by eq. (6), and the fitting parameters are Δε, α, β, and τ. The conductivity contribution (dc-conductivity) for the dielectric loss was described by the second term of eq. (6).

The conductivity, σ*(ω), the electric modulus, $M^*(\omega)$, and the loss tan δ are related with the

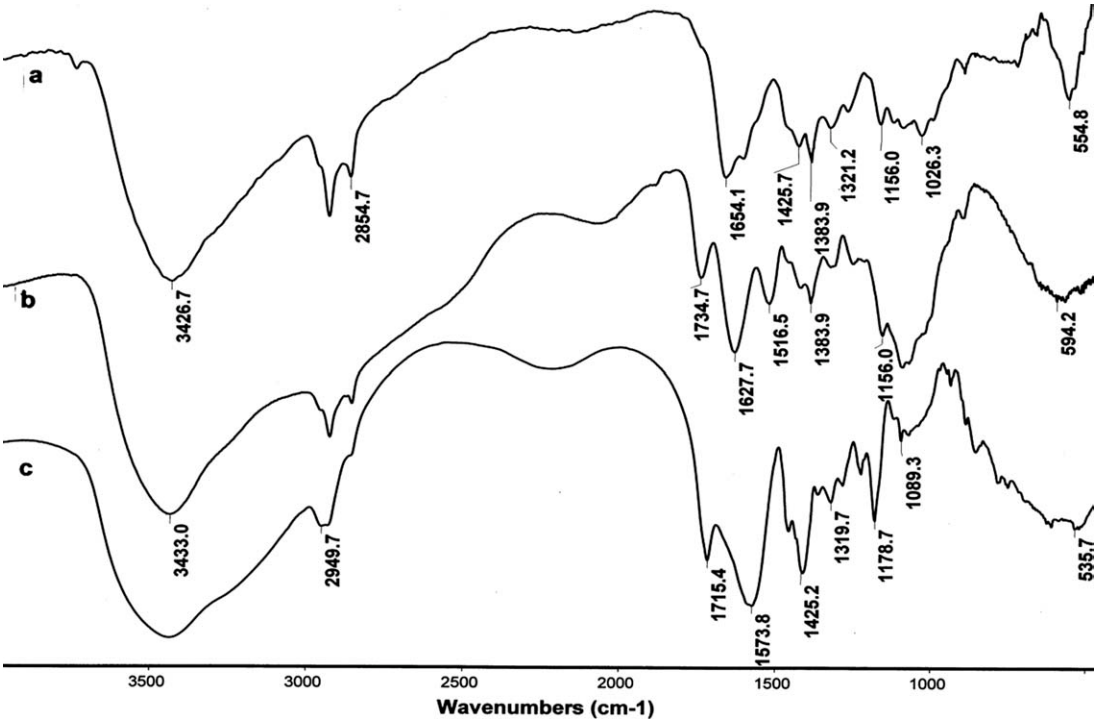

Figure 1 FTIR spectra for (a) Cs, (b) CMCs, and (c) CMCs-*g*-AAs.

dielectric function ε*(ω) through the following relationships:[37]

$$\sigma^*(\omega) = i\omega\varepsilon_0\varepsilon^*(\omega) = \sigma' + i\sigma'' \Rightarrow \sigma' = \omega\varepsilon_0\varepsilon'' \,, \sigma'' = \omega\varepsilon_0\varepsilon'$$

$$M^*(\omega) = \frac{1}{\varepsilon^*(\omega)} = M' + iM'' \Rightarrow\ M' = \frac{\varepsilon'}{\varepsilon'^2 + \varepsilon''^2},$$

$$M'' = \frac{\varepsilon''}{\varepsilon'^2 + \varepsilon''^2} \quad (8)$$

$$\tan\delta = \tan(90 - \phi) = \frac{\varepsilon''}{\varepsilon'}$$

where σ′ and σ″ are the real and imaginary parts of the conductivity, respectively, M' and M'' are the real and imaginary parts of the electric modulus, respectively, and φ is the phase angle. This representation is used to extract the ionic mobility from the crossing of the real (M') and the imaginary parts (M'') and the dc-conductivity from the plateau of the real part of the conductivity, σ′, at lower frequencies and elevated temperatures. Herein, the reported relaxation times are from the tan δ representation.

RESULTS AND DISCUSSION

Characterization of CMCs and CMCs-*g*-AAs copolymer

The CMCs was prepared by a method reported in an earlier study.[1] The Sd value of the CMCs was found to be 0.48 as determined by potentiometric titration and its intrinsic viscosity in 0.1*M* aqueous NaCl at 25°C was about 5.1 dL/g. The structural changes of Cs and its derivatives (CMCs and CMCs-*g*-AAs) were confirmed by FTIR (Fig. 1). The IR spectrum of Cs [Fig. 1(a)] shows a strong peak at 3427 cm^{-1} which is assigned to the N—H extension vibration, O—H stretching vibration, and the intermolecular H-bonds of the polysaccharide moieties. The weak peak at 1654 cm^{-1} is due to the amide C=O stretching. The IR spectrum of CMCs [Fig. 1(b)] shows a strong new peak at 1734 cm^{-1} representing the carboxylate C=O asymmetric stretching. The signal at 1384 cm^{-1} could be assigned to the symmetric stretching vibration of carboxylate C=O. The C—O absorption peak of the secondary hydroxyl group becomes stronger and moves to 1089 cm^{-1}. This tends to indicate that the substitution occurs mainly at the C_6 position. In case of IR spectrum of CMCs-*g*-AAs [Fig. 1(c)], the peak appeared at 1319 cm^{-1} is characteristic of poly(AAs). Also, in the IR spectra of the copolymer, the characteristic absorption peaks of polysaccharide at around 1100 cm^{-1} became weaker and that may be due to the high-grafting percentage. The IR spectrum of CMCs-*g*-AAs shows also the absence of clear absorption due to vinyl unsaturation around 1640 cm^{-1}. This tends to indicate the disappearance of the vinylic double bond of AAs monomer due to grafting. Various studies in literature have reported that the initiation site in this type of free radical-induced graft copolymerization onto CMCs backbone is the primary

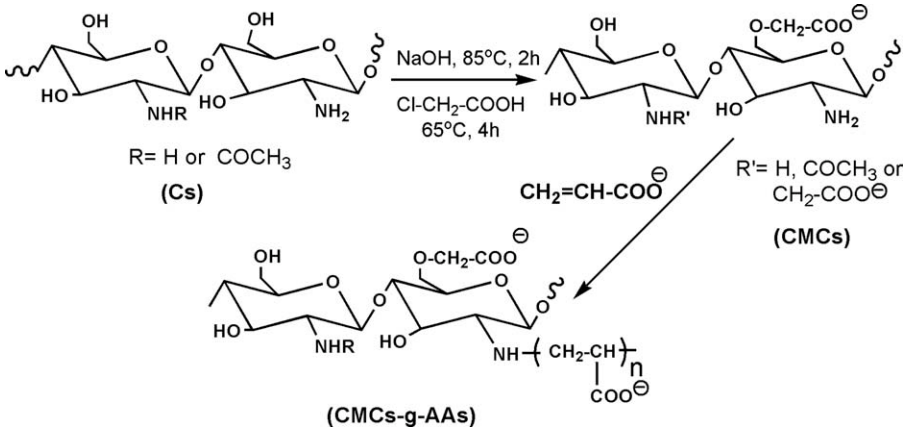

Scheme 1 Preparation of CMCs-*g*-AAs copolymer.

amino group on C_2 position[1,38] as illustrated in Scheme 1.

The occurrence of graft copolymerization was confirmed by several ways. For instance, the higher weight of the graft product as compared with that of the starting CMCs after the extensive removal of the homopolymer, poly(AAs) can be taken as evidence of grafting. The FTIR spectra of CMCs-*g*-AAs, as discussed above, had both characteristic peaks of CMCs and AAs, and this can be considered another experimental evidence of grafting. Also, as shown in Figure 2, the intensity of C=O absorption at about 1715 cm^{-1} was increased with increasing the *G*%. The incidence of grafting can also be deduced from the decreasing of *N*-content upon comparing the measured elemental analysis data of both CMCs and some CMCs-*g*-AAs copolymers (Table I).

Factors affecting grafting yield

Effect of initiator concentration

Figure 3 illustrates the effect of the initiator concentration, APS [m*M*] on the grafting degree. As appeared from the figure, with other reaction conditions kept constant, both *G*% and GE% increased with increasing the initiator concentration, in the range from 3 to 8 m*M*, reaching a maximum value, then decline again. From that, a relatively high concentration of the initiator may lead to a reduction of both *G*% and GE%. This behavior may be explained by a similar mechanism as proposed for grafting onto Cs by Li et al.[39] That is, with increasing the concentration of the initiator, more CMCs macroradicals are generated, thus more active sites of CMCs could react with AAs leading to increasing of *G*% and GE%. However, the excessive APS engendered a plenty of free radicals, which could terminate the propagation of graft copolymerization. This resulted in the decrease of *G*% and GE%. Moreover, at higher concentrations of APS, the formation of more homopolymer can be expected due to the nonavailability of sites on CMCs at which APS can generate free radicals on, and thus unutilized APS can lead to increase in the rate of homopolymerization.[18]

Effect of monomer concentration

The effect of monomer concentration on the yield of graft copolymerization is shown in Figure 4. It is apparent from the figure that there is an increase in both *G*% and GE% upon increasing the monomer concentration up to a certain value (2 m*M* of AAs

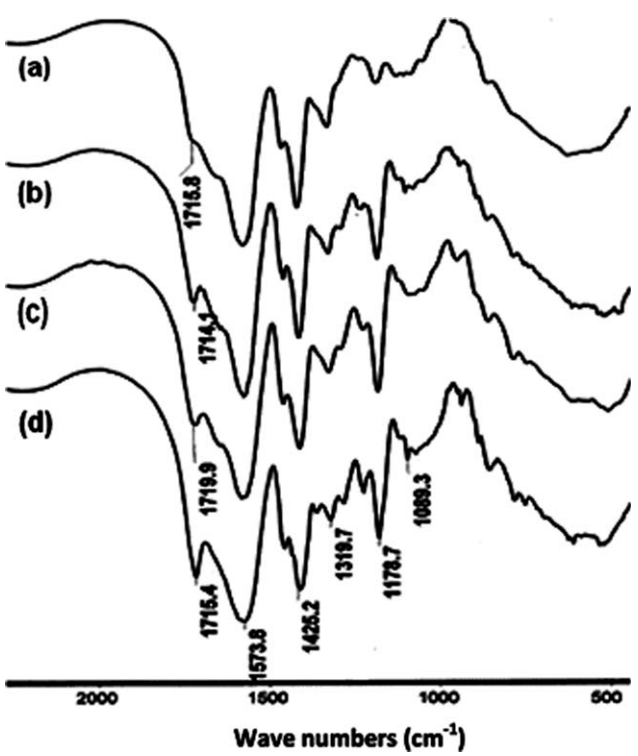

Figure 2 FTIR spectra of CMCs-*g*-AAs with different values of *G*%: (a) 400%, (b) 2390%, (c) 2900%, and (d) 3110%.

TABLE I
Some Characteristics of the Investigated CMCs, PAAs, and CMCs-*g*-AAs Copolymer Molecules

Sample code	*G*%	Elemental analysis data				XRD data for the investigated molecules			
		C (%)	N (%)	H (%)	O (%)	Δc_p (J g^{-1} K^{-1})	T_g (K)	*d* (nm)	2θ (°)	Phase
CMCs	–	37.21	5.11	5.85	51.83	11.88	481.64	0.20, 2.01, 2.21, 2.93, 3.18	45, 8.50, 6.44, ~ 5.5, 4.41, ~ 3.98, 3.21, 3.04, 2.82	Amorphous
Mb	400	33.62	0.65	4.77	60.96	4.97	487.78	<0.20, 0.71, 0.79, 2.01, 3.16	>45, 12.4, 11.2, 4.4, 2.8	Crystalline
Md	2390	31.44	0.30	4.74	63.52	1.58	475.16	<0.20, 0.79, 2.21, 2.97, 3.37, 3.48	>45, 11.15, 4.00, 2.98, 2.62, 2.54	Polycrystalline
Mf	2900	37.40	0.13	4.78	57.69	0.75	499.65	0.74, 2.16	11.9, 4.1	Semi-crystalline
Mg	3110	37.50	<0.10	4.79	57.61	0.53	501.10	0.76, 2.11	11.7, 4.2	Semi-crystalline
PAA	–	49.91	–	5.71	44.38	–	–	2.02	4.4	Highly amorphous

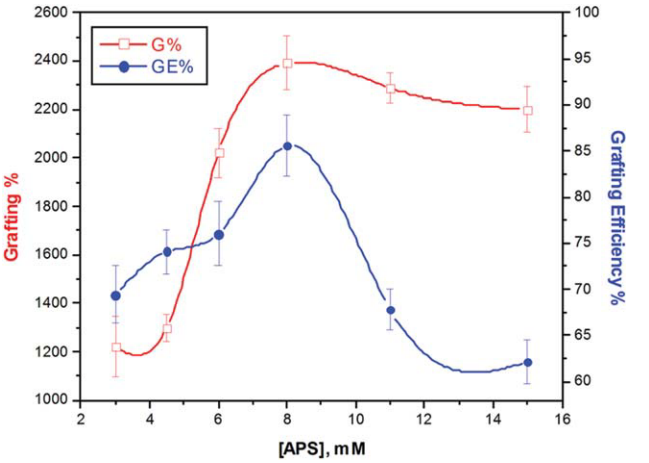

Figure 3 Effect of initiator concentration, [APS] on the grafting parameters; CMCs: 0.1 g; [AAs]: 2 m*M*; Time: 2 h; Temperature: 70°C. [Color figure can be viewed in the online issue, which is available at www.interscience.wiley.com.]

under the experimental conditions) and then they decrease gradually with the monomer further increasing. This phenomenon can be attributed to the limited number of active centers available for grafting on the polymer backbone then upon increasing the amount of monomer, more competition occurs between the monomer units for the same sites leading to increasing the grafting extent until saturation of the backbone. At higher concentrations of monomer, however, it seems that, the excess of monomer units induced much more chain transfer and termination reactions which led to more homopolymerization instead of grafting.

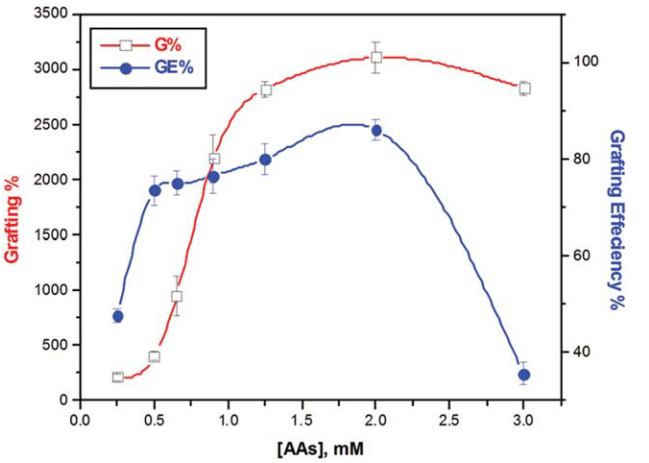

Figure 4 Effect of monomer concentration on the grafting parameters. CMCs: 0.1 g; [APS]: 8 m*M*; Time: 2 h; Temperature: 70°C. [Color figure can be viewed in the online issue, which is available at www.interscience.wiley.com.]

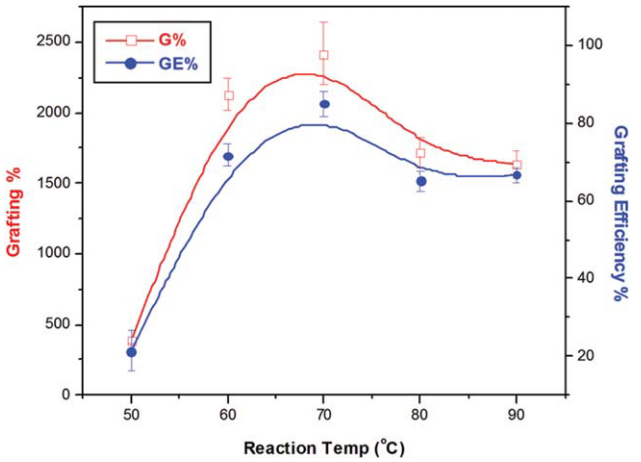

Figure 5 Effect of reaction temperature on the grafting parameters: CMCs: 0.1 g; [AAs]: 2 m*M*; [APS]: 8 m*M*; Time: 2 h. [Color figure can be viewed in the online issue, which is available at www.interscience.wiley.com.]

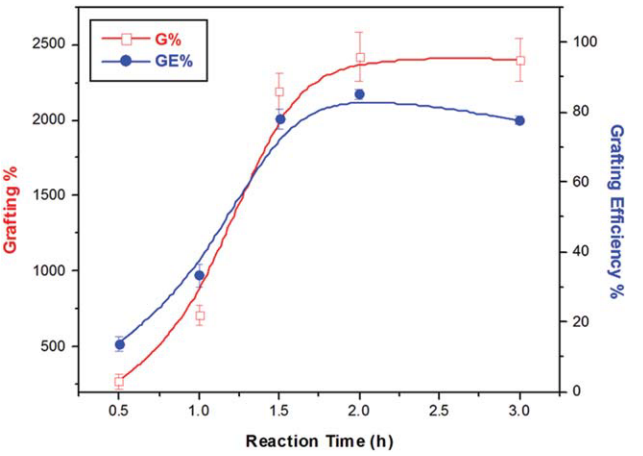

Figure 6 Effect of reaction time on the grafting parameters: CMCs: 0.1 g; [AAs]: 2 m*M*; [APS]: 8 m*M*; Temperature: 70°C. [Color figure can be viewed in the online issue, which is available at www.interscience.wiley.com.]

Effect of reaction temperature

The temperature effect on the grafting extent of AAs onto CMCs was investigated by changing the reaction temperature in the range from 50°C to 90°C as keeping the other reaction conditions constant. As apparent in Figure 5, both *G*% and GE% increase with increasing the reaction temperature form 50°C to 70°C, attain their optimum values at about 70°C and then decrease again with further rise in temperature. This dependence of grafting yield on reaction temperature may be attributed to the swelling of CMCs and the enhancement of the rate of diffusion of monomer. With further increase in temperature, the graft copolymerization may occur with a poor selectivity and various hydrogen abstraction and chain transfer reaction might be accelerated, and thus lead to a decrease in the grafting extent.[40]

Effect of the reaction time

Figure 6 illustrates the effect of reaction time on the grafting parameters. The influence of reaction time was investigated through checking the *G*% and GE% at different times from 0.5 to 3 h. Both *G*% and GE% increased with increasing the reaction time, and leveled off after about 2 h, reaching saturation value of grafting. This behavior is based on the fact that, as the reaction time increases, both the free radicals and amount of monomer in the reaction deduced leading to the leveling off the grafting parameters.

Structure investigation

Differential scanning calorimetry (DSC)

The traces from the second heating run for CMCs and the CMCs-*g*-AAs copolymers in the temperature range from 243 to 573 K are shown in Figure 7. A clear step in the specific heat can be seen at the glass transition temperature (T_g). The T_g was determined as the temperature of the mid point of the heat capacity increment in the transition. Samples codes, *G*%, specific heat (Δc_p) and T_g of the investigated molecules are compiled in Table I.

As appeared from the figure, the thermal behavior (DSC) of CMCs and the graft copolymers revealing the absence of a phase transformation within the investigated *T*-range. However, a clear step in the

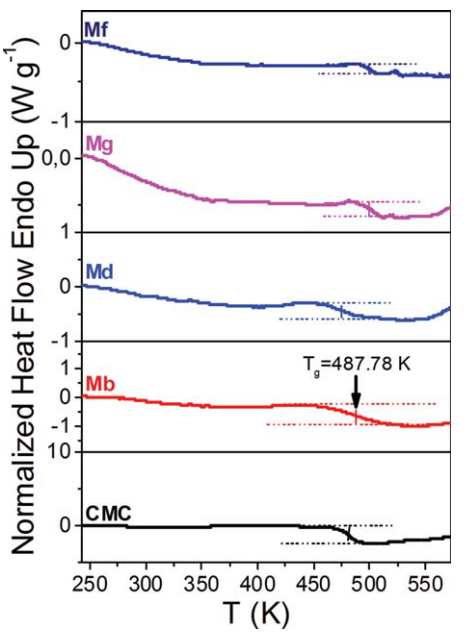

Figure 7 DSC trace of the CMCs and CMCs-*g*-AAs copolymers obtained during the second heating runs with a rate of 10 K min^{-1}. The vertical arrow indicates the respective glass transition temperature. [Color figure can be viewed in the online issue, which is available at www.interscience.wiley.com.]

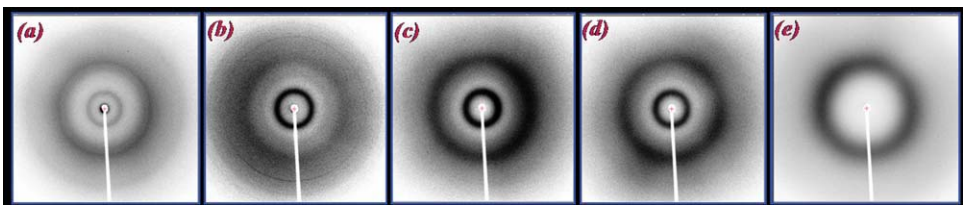

Figure 8 2D-WAXS images of the CMCs-*g*-AAs copolymers taken at $T = 298$ K. The sequence of the images is: (a) Mb, (b) Md, (c) Mf, (d) Mg, and (e) PAA. The images (a–e) represent crystalline, polycrystalline, semi-crystalline, semi-crystalline, and amorphous phases, respectively. [Color figure can be viewed in the online issue, which is available at www.interscience.wiley.com.]

specific heat can be seen at the glass temperature (T_g). Also, an abrupt change in the value of the heat capacity step (Δc_p) of the nongrafted polymer (CMCs) can be noticed upon grafting (Table I). Furthermore, the Δc_p of the graft copolymers tends to decrease with increasing the grafting (G%). The increase of the T_g upon grafting indicating that the CMCs backbone becomes more rigid due to the attachment of the acrylic acid side chains which causes slow down in mobility of the main chain.

Wide-angle X-ray scattering (WAXS)

The 2D-WAXS analysis of the powder samples were performed by using X-ray beam with a double graphite monochromator for the CuKα radiation (λ = 0.154 nm). Figure 8 illustrates some typical patterns for the investigated molecules given in Table I in addition to the PAA pattern.

The d-spacing values of the investigated molecules in the crystalline, semi-crystalline, and amorphous states were calculated from the scattering wave vector q (= $(4\pi/\lambda)\sin\theta$, 2θ is the scattering angle) according to the following relation:

$$d = \frac{2\pi}{q} \tag{9}$$

The scattering angles, 2θ, as well as the calculated d-spacing of the investigated molecules are shown in Table I.

The 2D-WAXS images shown in Figure 8 reveal that, at low grafting, as in the Mb and Md samples, a set of strong reflections appear indicating that these two samples exhibit crystalline and polycrystalline structures. With increasing grafting extent, as in the Mf and Mg samples, most of the reflection peaks disappeared, indicating that the samples had turned into semi-crystalline. The PAA shows only amorphous halo.

Surface morphology

Figure 9 illustrates the surface morphology of CMCs and CMCs-*g*-AAs copolymer. As may appear from the figure, the grafting process has turned the rough and irregular clusters of CMCs into different morphology with appearance of some microcrystalline aggregates which may return to the grafted AAs.

Molecular dynamics investigation

A copolymer sample with G% of 2900 (Mf) was selected, as example for other copolymers, to investigate its molecular dynamics using dielectric spectroscopy, DS (Table I). Figure 10 shows the result of the attempted time–temperature superposition (tTs) with respect to the loss tan δ data in the vicinity of the secondary relaxation, namely, the β-process. At each temperature, a single frequency-scale shift factor a_T and a single loss scale shift factor b_T allow the superposition of the different curves with the data at

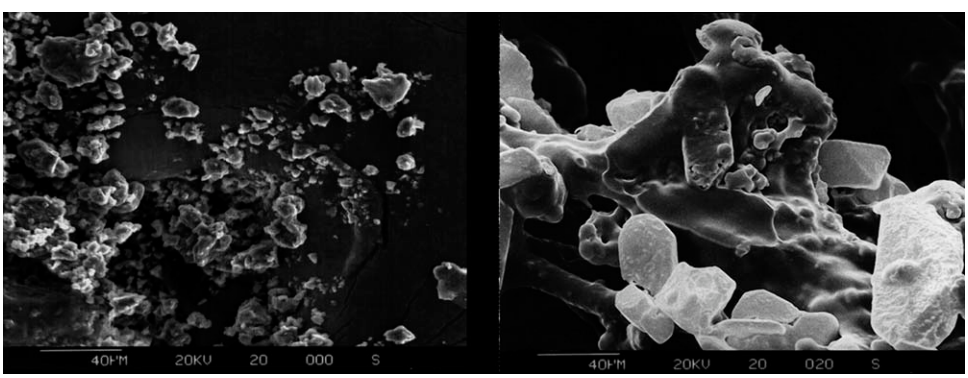

Figure 9 Scanning electron micrograph of (a) CMCs and (b) CMCs-*g*-AAs (Mb).

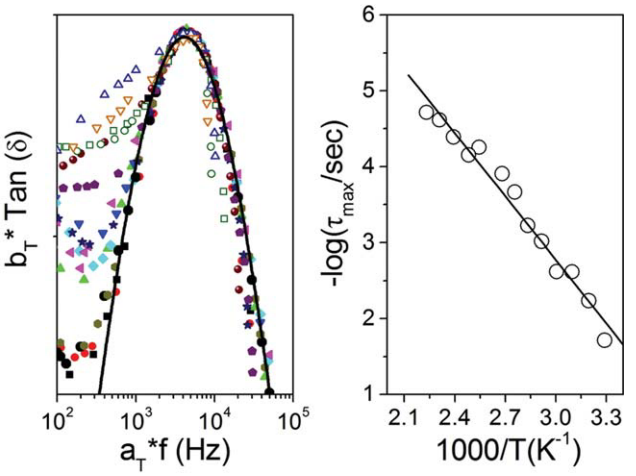

Figure 10 Left: Attempted time–temperature superposition (tTs) of the loss tan δ for the Mf sample β-process. The data points shown correspond to measurements within the temperature range 304–473 K. The reference temperature (●) is at 363 K. Loss tan δ data fit (solid line) to the HN eq. (6) (see text). The deviations at lower frequencies are due to the electrode polarization. Right: Arrhenius relaxation map for the β-process detected in the Mf sample. The solid line is fit to the Arrhenius equation and the fitting parameters are included in text.

the reference temperature 363 K. This procedure gives rise to the shown "master curve" with an extended frequency axis. The tTs is only approximately valid near the peak position. The shape of the loss peak deviates at lower frequencies due to the conductivity.

As illustrated in Figure 10, only one HN-function in addition to the conductivity contribution is able to describe the data of the loss tan δ of the dielectric function in the whole frequency range. The symmetrical (α) and asymmetrical (αγ) broadening parameters assumed values of $\alpha \sim \alpha\gamma \sim 0.62$. The shape of the loss peak deviates from a single Debye process ($\alpha = \alpha\gamma = 1$). The temperature dependence of relaxation times, $\tau(T)$, is shown in Figure 10 (Right) as a function of inverse temperature in the usual Arrhenius representation. The relaxation times of the β-process follow Arrhenius dependence[41,42]

$$\tau_{max} = \tau_0 \exp\left(\frac{E}{RT}\right) \tag{10}$$

with activation energy $E = 53 \pm 3$ kJ/mol and pre-exponential factor $\tau_0 = 7 \times 10^{-12}$ s characteristic of a local process (R is the gas constant). This relaxation process is related to a local main chain motion of CMCs coupled with adsorbed water. As previously mentioned, (see the Introduction) Einfeldt et al.[25,26] and Nogales et al.[28] reported the same relaxation process in Cs. The origin of the former finding (Einfeldt et al.) was attributed to the motion of a mixed phase of both polysaccharide and water, whereas the later (Nogales et al.) was attributed to hydrogen-bonded water.

The results of the DS investigation with respect to the ionic conductivity are better discussed with respect to the electric modulus and conductivity representations given by eq. (8). The electric modulus representation of the dielectric data allows extracting the ionic mobility. The characteristic relaxation times of the conductivity relaxation are obtained from the crossing of the real, M', and imaginary, M'', parts of the complex electric modulus function, M^* as illustrated in Figure 11.

The crossing point shifts to the high-frequency side with increasing temperature indicate that the ions are accelerated with increasing temperatures. The acceleration of ions with increasing temperature was recently reported by Elmahdy et al.[43] for a series of oligoindenofluorenes up to polymer.

The frequency-and temperature-dependence of the real part of the conductivity, σ′, of the Mf sample is characterized by a plateau at lower frequencies (dc-conductivity, σ_{dc}) and becomes strongly frequency dependent at higher frequencies ($\sigma'(\omega) \propto \omega^s$) as shown in Figure 12. This behavior can be further expressed by the following equation:[44,45]

$$\sigma'(\omega, T) = \sigma_{dc} + A\omega^s \tag{11}$$

where $0 < s \leq 1$ is a frequency exponent that depends on temperature and A is a constant that depends on temperature as well.

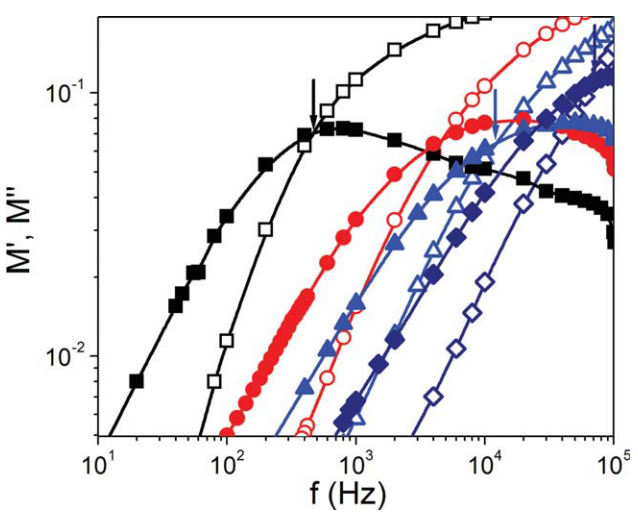

Figure 11 Real (open symbols) and imaginary (closed symbols) parts of the electric modulus for the Mf sample at 299 K (□,■), 313 K (○,●), 323 K (△,▲), and 353 K (◇,◆). The vertical arrows give the locations of the crossing of the real and imaginary parts. [Color figure can be viewed in the online issue, which is available at www.interscience.wiley.com.]

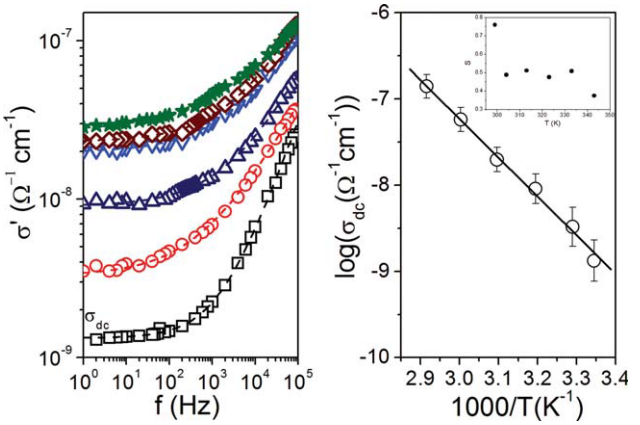

Figure 12 Left: The frequency dependence of the real part of the conductivity, σ′, of the Mf sample at different temperatures on heating: 299 K (□), 304 K (○), 313 K (△), 323 K (▽), 333 K (◇) and 343 K (★). Right: The temperature dependence of the dc-conductivity of the Mf sample on heating obtained from the fitting of the real part of the conductivity, σ′, by eq. (11). The inset shows the temperature dependence of the frequency exponent *s* obtained from the fitting of σ′ by eq. (11). [Color figure can be viewed in the online issue, which is available at www.interscience.wiley.com.]

The dc-conductivity, σ_{dc}, as well as the frequency exponent, *s*, is obtained from the fitting of the conductivity curves (Fig. 12) by eq. (11) at different temperatures. Figure 12 illustrates the temperature dependence of the σ_{dc} as a function of the inverse temperature. It has Arrhenius temperature dependence as follow:[46]

$$\sigma_{dc} = \sigma_0 e^{-\frac{E}{k_B T}} \quad (12)$$

where σ_0 is the pre-exponential factor (represents the dc-conductivity at infinite temperature), *E* is the activation energy of the process, k_B is the Boltzmann constant, and *T* is the absolute temperature of the sample. From the straight-line fitting, the value of the activation energy is $E = 86 \pm 9$ kJ/mol and the pre-exponential factor is $\sigma_0 = 5 \times 10^{-7}\ \Omega^{-1}\ cm^{-1}$. The activation energy value is in agreement with the values of 72.2 and 90.5 kJ/mol for wet and well dried starches, respectively.[24] The temperature dependence of the frequency exponent, *s*, is shown in the inset of Figure 12. From this figure, it is observed that, the frequency exponent, *s*, decreases monotonically from 0.76 to 0.37 in the temperature range of 299–343 K.

CONCLUSIONS

CMCs was prepared and then graft copolymerized with AAs. The grafting process was confirmed and the effects of reaction conditions on the grafting yield were studied. Then the structure and dynamic properties of the copolymers were investigated. The results of the 2D-WAXS revealed that, with increasing grafting percent the samples turned into semicrystalline. A detailed dielectric characterization has been made to CMCs-*g*-AAs sample with *G*%: 2900. One relaxation process with Arrhenius temperature dependence was observed. This process was related to local chain dynamics with activation energy of 53 ± 3 kJ/mol.

The authors are much indebted to Professor F. M. Reicha, Mansoura University, Egypt for helping with the dielectric measurements and also for Professor David R. K. Harding and Professor H. Smyth for facilitating some analysis of the prepared materials at Massey University, NZ and University of New Mexico, respectively.

References

1. El-Sherbiny, I. M. Eur Polym J 2009, 45, 199.
2. Jigar, M. J.; Sinha, V. K. Carbohydr Polym 2007, 67, 427.
3. Muzzarelli, R. A. A. Carbohydr Polym 1988, 8, 1.
4. Chen, L.; Du, Y.; Tian, Z.; Sun, L. J Polym Sci Part B: Polym Phys 2005, 43, 296.
5. Liu, Z.; Jiao, Y.; Zhang, Z. J Appl Polym Sci 2007, 103, 3164.
6. Terada, N.; Morimoto, M.; Saimoto, H.; Okamoto, Y.; Minami, S.; Shigemasa, Y. Chem Lett 1999, 28, 1285.
7. Sridhari, T. R.; Dutta, P. K. Indian J Chem Technol 2000, 7, 198.
8. Heras, A.; Rodriguez, N. M.; Ramos, V. M.; Agullo, E. Carbohydr Polym 2001, 44, 1.
9. Liu, Y. H.; Liu, Z. H.; Zhang, Y. Z.; Deng, K. L. J Macromol Sci Chem 2002, 39, 129.
10. Radhakumary, C.; Divya, G.; Nair, P. D.; Mathew, S.; Nair, C. P. R. J Macromol Sci Chem 2003, 40, 715.
11. Jenkins, D. W.; Hudson, S. M. Macromolecules 2002, 35, 3413.
12. Li, Y. P.; Liu, L.; Fang, Y. E. Polym Int 2003, 52, 285.
13. Joshi, J. M.; Sinha, V. K. J Polym Res 2006, 13, 387.
14. Joshi, J. M.; Sinha, V. K. Polymer 2006, 47, 2198.
15. Sun, T.; Xu, P.; Liu, Q.; Xue, J.; Xie, W. Eur Polym J 2003, 39, 189.
16. Zhu, A.; Zhang, M.; Zhang, Z. Polym Int 2004, 53, 15.
17. Xie, W.; Xu, P.; Liu, Q. Bioorg Med Chem Lett 2001, 11, 1699.
18. Joshi, J. M.; Sinha, V. K. Des Monomers Polym 2007, 10, 207.
19. Xie, W.; Xu, P.; Wang, W.; Liu, Q. J Appl Polym Sci 2002, 85, 1357.
20. Radloff, D.; Boeffel, C.; Spiess, H. W. Macromolecules 1996, 29, 528.
21. Montès, H.; Mazeau, K.; Cavaillè, J. Y. Macromolecules 1997, 30, 6977.
22. Meissner, D.; Einfeldt, L.; Einfeldt, J. J Polym Sci Part B: Polym Phys 2001, 39, 2491.
23. Butler, M. F.; Cameron, R. E. Polymer 2000, 41, 2249.
24. Einfeldt, J.; Maißner, D.; Kwasniewski, A.; Einfeldt, L. Polymer 2001, 42, 7049.
25. Einfeldt, J.; Maißner, D.; Kwasniewski, A. J Non-Cryst Solids 2003, 320, 40.
26. Einfeldt, J.; Maißner, D.; Kwasniewski, A. Prog Polym Sci 2001, 26, 1419.
27. Montès, H.; Cavaillè, J. Y. Polymer 1999, 40, 2649.
28. Nogales, A.; Ezquerra, T. A.; Rueda, D. R.; Martinez, F. J Colloid Polym Sci 1997, 275, 419.
29. Viciosa, M. T.; Dionísio, M.; Silva, R. M.; Reis, R. L.; Mano, J. F. Biomacromolecules 2004, 5, 2073.

30. Viciosa, M. T.; Dionísio, M.; Mano, J. F. Biopolymers 2006, 81, 149.
31. Roberts, G. A. F. Chitin Chemistry; MacMillan: Houndmills, 1992; p 274.
32. Ge, H. C.; Luo, D. K. Carbohydr Res 2005, 340, 1351.
33. Shantha, K. L.; Bala, U.; Panduranga, R. K. Eur Polym J 1995, 31, 317.
34. Pflugrath, J. W.; Acta Cryst 1999, D55, 1718.
35. Floudas, G. In Broadband Dielectric Spectroscopy; Kremer, F.; Schçnhals, A., Eds.; Springer: New York, 2002; Chapter 8.
36. Havriliak, S.; Negami, S. Polymer 1967, 8, 161.
37. McCrum, B. G.; Read, B. E.; Williams, G. Anelastic and Dielectric Effects in Polymeric Solids; Dover: New York, 1991.
38. Sabaa, M. W.; Mohamed, N. A.; Mohamed, R. R.; Khalil, N. M.; Abd El Latif, S. M. Carbohydr Polym 2010, 79, 998.
39. Li, W.; Li, Z. Y.; Liao, W. S.; Feng, X. D. J Biomater Sci Polym Ed 1993, 4, 557.
40. David, W. J.; Hudson, S. M. Chem Rev 2001, 101, 3245.
41. Blythe, A. R. Electrical Properties of Polymers; Cambridge University Press: New York, 1979.
42. Dyre, J. C. Rev Mod Phys 2006, 78, 953.
43. Elmahdy, M. M.; Floudas, G.; Oldridge, L.; Grimsdale, A. C.; Müllen, K. Chemphyschem 2006, 7, 1431.
44. Dyre, J. C. J Appl Phys 1988, 64, 2456.
45. Dyre, J. C.; Schröder, T. B. Rev Mod Phys 2000, 72, 873.
46. Davis, E. A.; Shaw, R. F. J Non-Cryst Solids 1970, 2, 406.